DOI:10.22337/2587-9618-2023-19-1-14-22

HYDRODYNAMIC STABILITY OF SWIRLING FLOWS WITH AXIAL RECIRCULATION ZONES

Vadim K. Akhmetov
Moscow State University of Civil Engineering, Moscow, RUSSIA

Abstact. The problem of the motion of a viscous incompressible swirling flow in an axisymmetric channel has been numerically investigated. Various flow regimes have been obtained, including those with the formation of the axial recirculation zones. In the framework of linear theory, the stability of the obtained calculated flows with respect to non-axisymmetric perturbations is investigated on the assumption of local parallelism. The growth rates and phase velocities of unstable disturbances are calculated. In the presence of a reverse flow zone, the disturbances growth rates are increased significantly.

Keywords: theory of hydrodynamic stability, swirling flows, growth rates factors, phase velocities

ГИДРОДИНАМИЧЕСКАЯ УСТОЙЧИВОСТЬ ЗАКРУЧЕННЫХ ПОТОКОВ С ПРИОСЕВЫМИ ЗОНАМИ РЕЦИРКУЛЯЦИИ

В.К. Ахметов
Национальный исследовательский Московский государственный строительный университет, г. Москва, РОССИЯ

Аннотация. Численно исследована задача о движении закрученного потока вязкой несжимаемой жидкости в осесимметричном канале. Получены различные режимы течений, в том числе с образованием приосевых рециркуляционных зон. В рамках линейной теории на основе гипотезы локальной параллельности потока исследована задача об устойчивости полученных расчетных течений по отношению к неосесимметричным возмущениям. Рассчитаны коэффициенты усиления и фазовые скорости неустойчивых возмущений. При наличии в потоке зоны возвратного течения коэффициенты усиления возмущений существенно возрастают.

Ключевые слова: гидродинамическая теория устойчивости, закрученные течения, коэффициенты усиления, фазовые скорости

1. INTRODUCTION

Swirling flows have a wide area of applications in various technical field. They are used to intensify heat and mass transfer processes, purify gases and liquids from impurities, stabilize combustion processes, extinguish energy in hydraulic structures, and etc. The swirl has a significant effect on all the main characteristics of the flow, including its stability. In this case, a critical point (stagnation point) with zero velocity is formed on the flow axis or near it. Behind of this point, a reverse flow zone is formed. The emerging instability leads to the formation of secondary vortex motions, and can also be the cause of the collapse of the vortex.

The phenomenon of collapse (destruction) of a vortex (vortex breakdown) was first discovered in aerodynamic studies during the flow around the wings of a large sweep. Disturbances of the vortex decay type are characterized by a sudden deviation of the vortex axis from its original direction or a sharp increase in the vortex core.
The existing results on the study of vortex decay are systematized in review [1]. Most of the experiments were carried out in weakly expanding axisymmetric tubes. Currently, eight types of vortex decay have been recorded. Their detailed classification is presented in [2]. Two types of vortex breakdown are most common: bubble breakdown and spiral breakdown. Bubble breakup is characterized by a critical point on the flow axis, followed by an almost axisymmetric shell of

the recirculation zone. In problems related to combustion, such recirculation regions serve as a kind of flame holder [3]. In other technical devices such as presented [4, 5], the formation of counter flow zones is undesirable, since it can lead to excessive deceleration of the main flow. After axisymmetric decay, as a rule, spiral decay follows. Although, they can be observed independently. Spiral decay is characterized by a sharp break in the vortex axis, after which a corkscrew-like swirling of the flow occurs.

Thus, when the vortex is destroyed, a significant rearrangement of the initial flow occurs. In particular, it was experimentally established [6] that after the collapse of a vortex, the flow, as a rule, becomes turbulent.

The phenomenon of vortex decay is closely related to the development of flow instability. The problem of the stability of a free vortex whose velocity profiles can be obtained from the self-similar Batchelor solution for a viscous swirling wake was studied in [7–12]. In the paper [9], selective calculations were performed for the first three instability modes of a free vortex. And a new viscous instability mode was discovered for the first time. Detailed studies of that are presented in [10]. In the paper [11], the instability of the flow under study was presented for large values of the swirling parameter of the flow. There, the existence of up to eight unstable modes simultaneously was established. The branching of eigensolutions is discovered and the filling of the region of admissible values in the space of free parameters by instability modes is studied.

The paper [12] provides a study on the stability of a swirling flow in an unbounded medium, the velocity profiles of which were obtained by numerically solving the complete system of Navier–Stokes equations. This study was based on the hypothesis of local parallelism of the flow. It is shown that in the presence of a recirculation zone in the flow, the strongest instability was observed. The oscillation frequencies corresponding to the most unstable wavenumber are consistent with the results on the stability of vortices coming off the trailing edge of an aircraft wing and with research data on the spectral characteristics of swirling flows in an expanding channel [13].

This paper aims to study the problem of the stability of an internal swirling flow in an axisymmetric channel, using a similar approach.

2. STATEMENT OF THE PROBLEM ON THE MOTION OF A SWIRLING FLOW

The paper considers the problem of the development of a swirling flow in an axisymmetric channel of radius. Axisymmetric laminar flows of a viscous incompressible fluid are described by the Navier–Stokes system of equations. In a cylindrical coordinate system r, φ, z with respect to the stream function ψ, the vorticity Ω and the azimuthal velocity V_φ can be represented as follows

$$\frac{1}{r}\frac{\partial^2\psi}{\partial z^2}+\frac{\partial}{\partial r}\left(\frac{1}{r}\frac{\partial\psi}{\partial r}\right)=-\Omega \tag{1}$$

$$\frac{\partial\Omega}{\partial t}+\frac{\partial}{\partial z}(V_z\Omega)+\frac{\partial}{\partial r}(V_r\Omega)= =\frac{1}{\mathrm{Re}}\left[\frac{\partial^2\Omega}{\partial z^2}+\frac{\partial^2\Omega}{\partial r^2}+\frac{\partial}{\partial r}\left(\frac{\Omega}{r}\right)\right]+G^2\frac{1}{r}\frac{\partial(V_\varphi)^2}{\partial z} \tag{2}$$

$$\frac{\partial V_\varphi}{\partial t}+\frac{\partial}{\partial z}(V_zV_\varphi)+\frac{1}{r}\frac{\partial}{\partial r}(rV_rV_\varphi)+\frac{V_rV_\varphi}{r}= =\frac{1}{\mathrm{Re}}\left[\frac{\partial^2V_\varphi}{\partial z^2}+\frac{1}{r}\frac{\partial}{\partial r}\left(r\frac{\partial V_\varphi}{\partial r}\right)-\frac{V_\varphi}{r^2}\right] \tag{3}$$

$$V_r=-\frac{1}{r}\frac{\partial\psi}{\partial z},\quad V_z=\frac{1}{r}\frac{\partial\psi}{\partial r},\quad \Omega=\frac{\partial V_r}{\partial z}-\frac{\partial V_z}{\partial r} \tag{4}$$

The system of equations (1)–(4) is written in a conservative dimensionless form. The axial V_z and radial V_r velocities are related to the characteristic value U_0. The azimuthal velocity V_φ is related to the characteristic value W_0. The coordinates are related to the radius r_0, and the time is related to the value r_0/U_0. The system of equations (1)–(4) contains two dimensionless parameters:

Reynolds number $\mathrm{Re} = U_0 r_0 / \nu$, in which ν is the kinematic viscosity, and spin parameter is $G = W_0 / U_0$.

The solution of the problem under consideration is determined in the area D: $0 \le z \le z_k$, $0 \le r \le 1$. At the input $z = 0$, the following distributions for the axial and azimuthal velocity components (the radial velocity in the initial section is assumed to be zero) were set:

$$\begin{aligned} &V_{z0}(r) = D_0 + D_1 \exp(-B_1 r^2), \\ &V_{\varphi 0}(r) = \frac{A}{r}(1 - \exp(-B_2 r^2)), \ 0 \le r \le r_0, \\ &V_{z0}(r) = a_0 + a_1 r + a_2 r^2, \\ &V_{\varphi 0}(r) = b_0 + b_1 r + b_2 r^2, \qquad r_0 \le r \le 1. \end{aligned} \tag{5}$$

These profiles are consistent with experiments [6]. For $0 \le r \le r_0$, the distribution of velocities (5) corresponds to a free vortex. The constant B_2 characterizes the value r at which the azimuth velocity is maximum. By selecting D_0, D_1, a corollary or jet type flow can be gotten. In the equations (5), the coefficients of the polynomials a_i, b_i are found from the no-slip conditions at 1 and the continuity of the velocities $V_{z0}(r)$, $V_{\varphi 0}(r)$, and their derivatives at the point r_0.

The set of boundary conditions, including setting velocity profiles $V_{z0}(r)$, $V_{\varphi 0}(r)$ at the input $z = 0$, no-slip conditions on the channel walls, symmetry conditions on the axis $r = 0$, and soft boundary conditions in the outlet section $z = z_k$, for this problem can be represented as:

$$\begin{aligned} &\psi = \psi_0(r), V_\varphi = V_{\varphi 0}(r), \frac{\partial \psi}{\partial z} = 0, \ 0 \le r \le 1, \ z = 0 \\ &\psi = \psi_0 = \mathrm{const}, V_\varphi = 0, \frac{\partial \psi}{\partial r} = 0, \ 0 \le z \le z_k, \ r = 1 \\ &\psi = 0, V_\varphi = 0, \Omega = 0, \ 0 \le z \le z_k, \ r = 0 \\ &\frac{\partial \psi}{\partial z} = \frac{\partial \Omega}{\partial z} = \frac{\partial V_\varphi}{\partial z} = 0, \quad 0 \le r \le 1, \quad z = z_k \end{aligned} \tag{6}$$

For the numerical solution of the boundary value problem (1)–(4) with boundary conditions (6), the finite difference method was used, which was tested and successfully applied in [14–17] to calculate swirling flows of various types. In these calculations, the following values were accepted:

$$\begin{aligned} &D_0 = 1, \ D_1 = 0, \ B_1 = 0, \ B_2 = 14, \\ &A = 0.419, \ r_0 = 0.75, \ z_k = 10 \end{aligned} \tag{7}$$

3. RESULTS

The calculations of the flow fields corresponding to the boundary value problem (1) – (4), (6), (7) were carried out at $\mathrm{Re} = 100$, 150, 300, 500 in the swirl range $0 \le G \le 3$. The most characteristic patterns of streamlines are shown in Fig.1. Further, the main properties of the calculated flows are considered in detail.

At a sufficiently large swirl value (depending on the value of the number Re), a reverse flow zone appears in the axial part of the channel, limited by stagnation points (z_1, z_2) located on the symmetry axis. This recirculation region has a toroidal structure with closed current lines. An example of such a flow at $\mathrm{Re} = 100$, $G = 2.1$ is shown in Fig.1, b. As the swirl increases, the diameter d_0 of the return flow region increases, the recirculation region shifts upstream, and the rear stagnation point z_2 slightly shifts towards the front one z_1.

If Reynolds number is higher of 150, G= 2.2, the return flow region is formed somewhat closer to the input section and its length in the direction z decreases (Fig. 1, c). With an increase in swirl G=2.4, the rear stagnation point approaches the anterior one, and the streamlines behind the recirculation zone acquire a zigzag shape. With a further increase in swirl G=2.6 (figure 1, d) downstream of the first region of the return flow, a second recirculation zone is formed. It also has a toroidal structure, but with a lower recirculation rate and a smaller diameter. The length of the

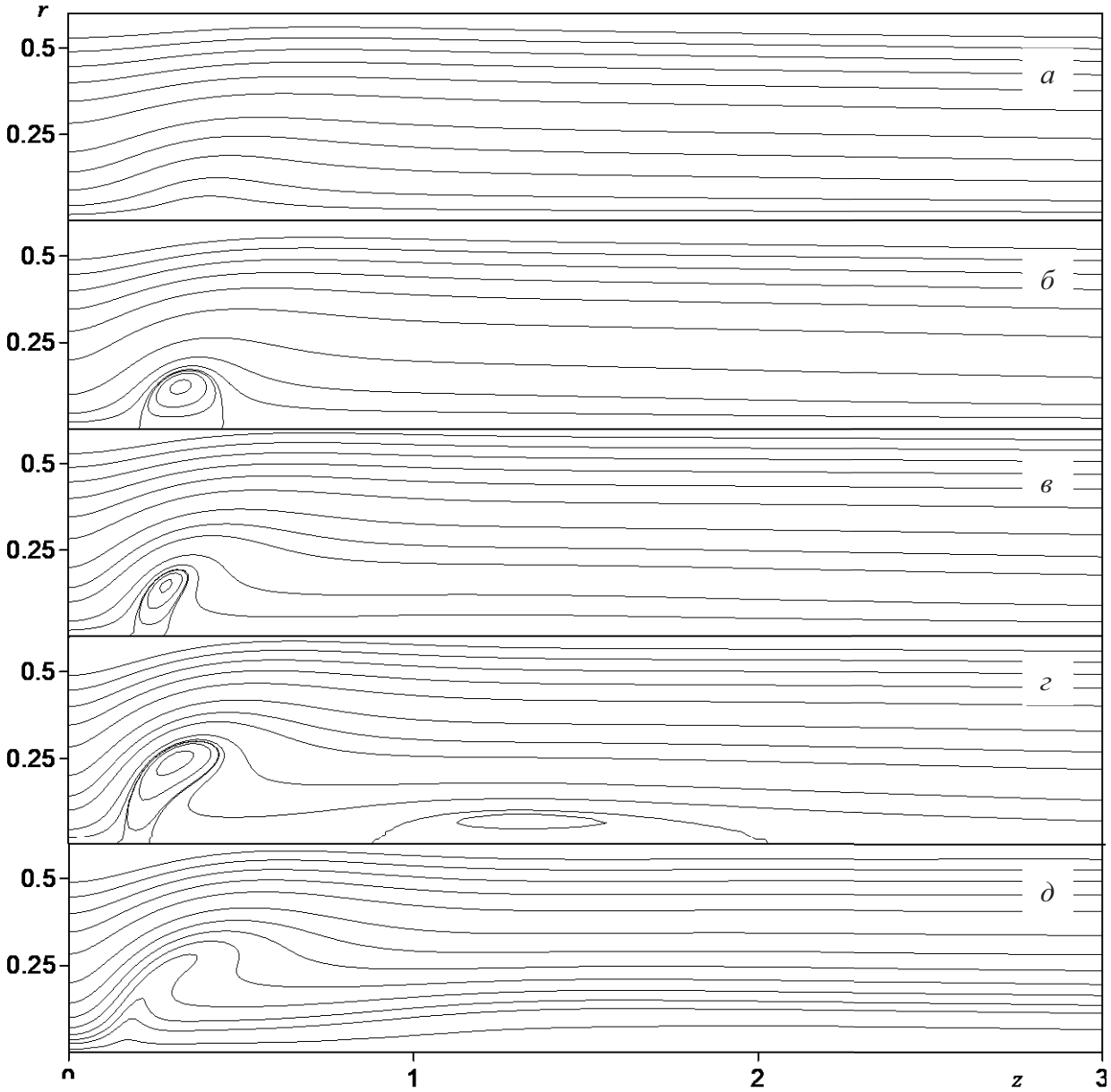

Figure 1. Streamlines for Re=100, G=1.7 (а), G=2.1 (б); Re=150, G=2.2 (в), G=2.6 (г); Re=300, G=2.4 (д)

second reverse flow zone is much longer than the first.

A further increase in the Reynolds number Re=300 leads to a qualitative change in the flow pattern. With a sufficiently high swirl 2.4 (Fig.1, e), the first recirculation zone on the channel axis is not formed (the flow directly in the axial part for $r \le 0.05$ moves forward). In contrary, a separation region with a reverse flow is formed at a distance of $r \approx 0.1$–0.3 from the symmetry axis.

4. FLOW STABILITY

Further, the small perturbations of a swirling flow with given velocity profiles are considered

$$V_z = U(r), \qquad V_\varphi = W(r), \qquad V_r = 0 \qquad (8)$$

as solutions of the linearized Navier–Stokes equations of the traveling wave type (normal modes)

$$\{V_z', V_r', V_\varphi', p'\} = \\ = \{F, iS, H, P\}\exp[i(\alpha z + n\varphi - \alpha ct)], \quad (9)$$

in which p is the pressure; alpha is the wave number; n is the perturbation mode $(n = 0; \pm 1; \pm 2; ...)$; c is the speed of wave propagation; i is an imaginary unit. For complex amplitude functions F(r), S(r), H(r), P(r) a system of equations are obtained:

$$r^2\gamma F + \alpha r^2 P + r^2 SU' = \\ = \frac{1}{i\,\mathrm{Re}}\left[r\left(rF'\right)' - \left(\alpha^2 r^2 + n^2\right)F\right],$$

$$r^2\gamma S + 2rHW - r^2 P' = \\ = \frac{1}{i\,\mathrm{Re}}\left[r\left(rG'\right)' - \left(\alpha^2 r^2 + n^2 + 1\right)S - 2nH\right], \quad (10)$$

$$r^2\gamma H + r^2 S\left(W' + \frac{W}{r}\right) + rnP = \\ = \frac{1}{i\,\mathrm{Re}}\left[r\left(rH'\right)' - \left(\alpha^2 r^2 + n^2 + 1\right)H - 2nS\right],$$

$$\alpha rF + \left(rS\right)' + nH = 0,$$

where $\gamma = \alpha(U - c) + nW/r$. Prime means a derivative with respect to r. For system (10) at r = 0, the boundary conditions are derived from the requirements for the regular behavior of the solution near the axis and have the form

$$S(0) = H(0) = 0, \\ F(0), P(0) - \textit{restricted for } n = 0; \\ S(0) \pm H(0) = 0, \\ F(0) = P(0) = 0 - \text{при } n = \pm 1; \quad (11) \\ S(0) = H(0) = F(0) = P(0) = 0 - \textit{for } |n| > 1; \\ S(1) = H(1) = F(1) = 0.$$

Let's consider perturbations (9) periodic in z, whose amplitude varies with time. Then α is a real number ($\alpha = 2\pi/\lambda$, where λ is the perturbation wavelength), and $c = c_r + ic_i$ is the complex one; c_r is the velocity of propagation of the perturbation in the direction z (phase velocity), c_i is the rate of rise of the perturbation in time, $\omega_i = \alpha c_i$ is the amplification factor of the perturbations, and $\omega_r = \alpha c_r$ is the oscillation frequency. For $c_i < 0$, the perturbation amplitudes (9) decay (the flow is stable), and for $c_i > 0$, they increase with time (the flow is unstable).

The method for calculation of eigenvalues is described in [9-10], and testing of the method is presented in [11].

For the calculated swirling flows, the maximum value of the radial velocity component is smaller over order than the corresponding values for the axial and azimuthal components. In the distributions $V_z(r,z)$, $V_\varphi(r,z)$, the relation with z is significantly manifested only in the very initial section near the inlet section. Therefore, the problem of the stability of the obtained flows with respect to non-axisymmetric perturbations (9) at r=-1 is considered under the assumption that the flow is locally parallel. For this purpose, in the system of equations (10) take profiles $V_z(r,z_0)$, $V_\varphi(r,z_0)$ as $U(r)$, $W(r)$, from calculations in the system of equations (10). Here z_0 is a parameter.

First, the case was studied, for which the initial swirling of the flow is insufficient to form a reverse flow zone. Only a slight swelling of the streamlines is observed in the axial part of the flow. An example of such a flow at Re=100, G=1.7 is shown in figure 1, a. Figure 2, a show the dependences of the gains ω_i and the corresponding phase velocities ω_r on the wave number α obtained in different cross sections of the flow z=const for this case. In the initial section z=0 (curve 1), a very slight flow instability is observed with a maximum value of $\omega_i^* = \max\omega_i = 0.0027$ in a narrow range of the wave number $3.18 \le \alpha \le 3.55$. In the next section, at z=0.31 (curve 2), the instability increases and at z=2.5 (curve 4) it becomes the largest. Further downstream, the instability

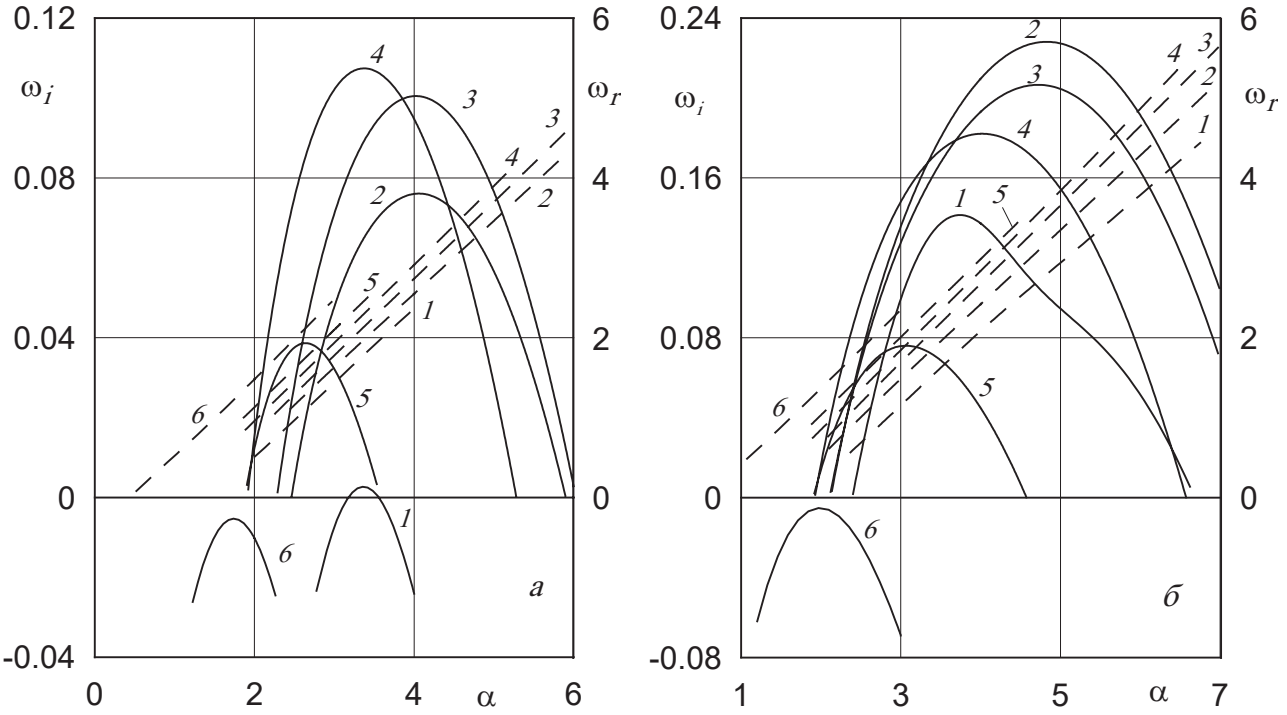

Figure 2. Amplification factors - wave number (_____) and oscillation frequency - wave numbers (_ _ _) diagrams for добавить Re и G ..... in the sections z=0, 0.31, 0.62, 2.5, 5, 10 (curves 1-6)

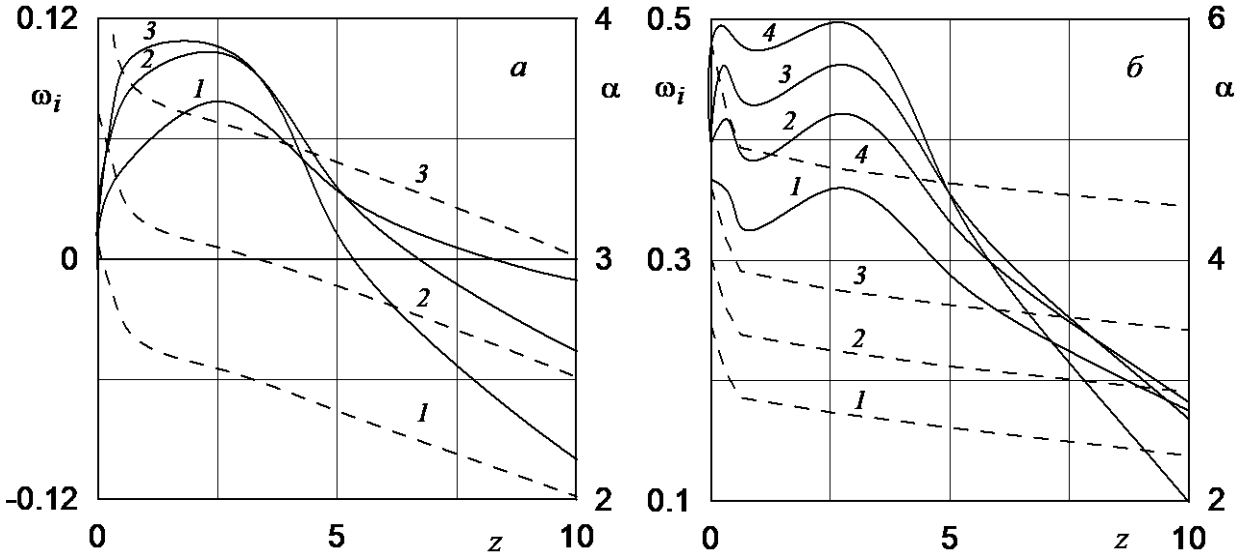

Figure 3. Amplification factors - axis coordinate (_____) and wave numbers – axis coordinate (_ _ _) diagrams for добавить *Re* и *G* ..... for fixed oscillation frequencies

decreases, and at z=10 (curve 6) at the channel outlet, the flow becomes stable ($\omega_i < 0$).

Figure 3, a show the change in amplification factors ω_i and wave numbers α along the flow axis for perturbations (9) with a fixed oscillation frequency ω_r. All diagrams $\omega_i(z)$ show a local maximum at $z \approx 2.5$.

Thus, swirling of the flow leads to instability of the flow before the formation of the recirculation zone. The axial velocity profiles in this case are characterized by a large velocity defect on the ($V_* \approx 0.1$) axis, have an inflection

point at $z \approx 0.25$, and differ significantly from the parabolic distribution.

At Re=100, G=2.1, there is a paraxial zone of reverse stream in the flow at $0.207 \le z \le 0.448$ (figure 1, b). The calculated amplification factors and oscillation frequencies for a given flow are shown in Fig.2, b. In the initial section z=0 (curve 1), the flow is unstable with a maximum amplification factor of $\omega_i^* = 0.141$ at $\alpha_* = 3.74$. In the region of the reverse flow at z=0.31 (curve 2), the strongest instability is noted. At $0.6 \le z \le 2.5$, the maximum values of the amplification factors change insignificantly. Further downstream, the instability decreases and at the outlet at z=10 (curve 6), the flow becomes stable ($\omega_i < 0$).

Таким образом, закрутка потока приводит к неустойчивости

Characteristic relations for the change in the amplification factors along the flow axis for flows with a recirculation zone are shown in Fig.3, b. The distribution $\omega_i(z)$ has two local maxima. One of them at $z \approx 2.5$ is observed in all calculated unstable flows and is associated with the swirl effect. The other, located upstream at $z \approx 0.3$, is due to the presence of a reverse flow zone in the flow. The values of the amplification factors at the points of local maxima are close to each other. In contrast to the flow without the formation of a recirculation zone, the velocity V_z profiles in the axial region have two inflection points at $r \approx 0.1$; 0.3. As can be seen from figures 3, a, b, the values of the wavelengths corresponding to the most growing disturbances in the first and second zones differ insignificantly.

At Re=150 or more intense initial swirl G=2.6 in the flow, a second axial region of the return flow is formed (figure 1, d). It has a large length along z, and the recirculation rate is less. In this case, the distribution $\omega_i(z)$ is completely similar to the previous case and has two local maxima, each of which is observed in the region of the reverse flow zones. Moreover, instability in the first recirculation zone leads to the formation of a more pronounced maximum for the second zone.

The results obtained are consistent with the calculations of the spatiotemporal instability of swirling flows in an unbounded medium [18, 19], which show that the strongest flow instability is observed in the region of bubble-like decay and in its wake with the formation of a spiral form of decay.

5. CONCLUSION

The provided studies on the swirling flows show that there are two mechanisms of instability. The first one is related with the effect of flow swirl, the second one with the formation of reverse flow zones. The traveling wave of perturbations successively passes through two zones, in which its amplitude grows most rapidly. This effect can contribute to the destruction of the vortex.

REFERENCES

1. **Lucca-Negro O., O'Doherty T.** Vortex breakdown: a review // Progr. in Energy and Comb. Sci. 2001. V. 27. P. 431-481.
2. **Alekseenko S.V., Kuibin P.A., Okulov V.L.** Introduction to theory of concentrated vortices. Moskow–Izhevsk: Institute of Computer Science. 2005. 504 p.
3. **Gupta A.K, Lilley D.G, Syred N.** Swirl Flows 1984 (Abacus Press)
4. **Akhmetov V.K., Shkadov V.Ya., Konon P.N.** Aerodynamics of building structures for flue gas removal. Magazine of Civil Engineering. 2018. 81(5). Pp. 81-92.
5. **Akhmetov V.K.** Method of effective parameters for calculations of turbulent swirling flows in engineering constructions // IOP Conf. Series: Materials Science and Engineering. 2020. V. 869. 052020.
6. **Faler J.H., Leibovich S.** An experimental map of the internal structure of a vortex

breakdown // J. Fluid Mech. 1978. V. 86. № 2. P. 313-335.
7. **Lessen M., Paillet F.** The stability of a trailing line vortex. Part 2. Viscous theory // J. Fluid Mech. 1974. V. 65. Pt. 4. P. 769-779.
8. **Mayer E.W., Powell K.G.** Viscous and inviscid instabilities of a trailing vortex // J. Fluid Mech. 1992. V. 245. P. 91-114.
9. **Akhmetov V.K., Shkadov V.Ya.** Stability of a free vortex // Moscow University Mechanics Bulletin. 1987. V. 42. № 2. P. 17-22.
10. **Akhmetov V.K.** Structure and branching of unstable modes in a swirling flow // Mathematics. 2022. V.10(1). 99.
11. **Akhmetov V.K., Shkadov V.Ya.** Instability of a free vortex for large swirl numbers // Moscow University Mechanics Bulletin. 2003. T. 58. № 1. C. 23-27.
12. **Akhmetov V.K.** Development and stability of swirling flows // Fluid Dynamics. 1988. V. 23. № 4. P. 485-492.
13. **Garg A.K., Leibovich S.** Spectral characteristics of vortex breakdown flowfields // Phys. Fluids. 1979. V. 22. P. 2053-2064.
14. **Akhmetov V.K.** Numerical and asymptotic flow stability analysis of vortex structures // E3S Web of Conferences. 2021. V. 263. 03003.
15. **Akhmetov V.K., Shkadov V.Ya**. Atomization of a powder by a swirling flow with a recirculation zone // Fluid Dynamics. 2000. V. 35. № 6. P. 791-802.
16. **Akhmetov V.K., Akhmetova V.V.** Mathematical Modelling of Vortex Dust Separator // IOP Conf. Series: Materials Science and Engineering. 2019. 661.
17. **Akhmetov V.K., Medvedev Yu.V., Shkadov V.Ya.** Effect of the Inertia Terms in Sliding Bearing Calculation Problems // Fluid Dynamics. 2014. Vol.49. №3. P.320-329.
18. **Herrada M. A., R. Fernandez-Feria R.** On the development of three-dimensional vortex breakdown in cylindrical regions // Phys. Fluids. 2006. V. 18. 084105. 15 p.
19. **Gallaire F., Ruith M., Meiburg E., Chomaz J., Huerre P.** Spiral vortex breakdown as a global mode // J. Fluid Mech. 2006. V. 549. P. 71-80.

СПИСОК ЛИТЕРАТУРЫ

1. **Lucca-Negro O., O'Doherty T.** Vortex breakdown: a review // Progr. in Energy and Comb. Sci. 2001. V. 27. P. 431-481.
2. **Алексеенко С.В., Куйбин П.А., Окулов В.Л.** Введение в теорию концентрированных вихрей. Москва–Ижевск: Институт компьютерных исследований, 2005. 504 с.
3. **Гупта А., Лилли Д., Сайред Н.** Закрученные потоки. М.: Мир, 1987. 588 с.
4. **Ахметов В.К., Шкадов В.Я., Конон П.Н.** Аэродинамика строительных сооружений для удаления дымовых газов // Инженерно-строительный журнал. 2018. № 5(81). С. 81-92.
5. **Akhmetov V.K.** Method of effective parameters for calculations of turbulent swirling flows in engineering constructions // IOP Conf. Series: Materials Science and Engineering. 2020. V. 869. 052020.
6. **Faler J.H., Leibovich S.** An experimental map of the internal structure of a vortex breakdown // J. Fluid Mech. 1978. V. 86. № 2. P. 313-335.
7. **Lessen M., Paillet F.** The stability of a trailing line vortex. Part 2. Viscous theory // J. Fluid Mech. 1974. V. 65. Pt. 4. P. 769-779.
8. **Mayer E.W., Powell K.G.** Viscous and inviscid instabilities of a trailing vortex // J. Fluid Mech. 1992. V. 245. P. 91-114.
9. **Akhmetov V.K., Shkadov V.Ya.** Stability of a free vortex // Moscow University Mechanics Bulletin. 1987. V. 42. № 2. P. 17-22.

10. **Akhmetov V.K.** Structure and branching of unstable modes in a swirling flow // Mathematics. 2022. V.10(1). 99.
11. **Akhmetov V.K., Shkadov V.Ya.** Instability of a free vortex for large swirl numbers // Moscow University Mechanics Bulletin. 2003. T. 58. № 1. C. 23-27.
12. **Akhmetov V.K.** Development and stability of swirling flows // Fluid Dynamics. 1988. V. 23. № 4. P. 485-492.
13. **Garg A.K., Leibovich S.** Spectral characteristics of vortex breakdown flowfields // Phys. Fluids. 1979. V. 22. P. 2053-2064.
14. **Akhmetov V.K.** Numerical and asymptotic flow stability analysis of vortex structures // E3S Web of Conferences. 2021. V. 263. 03003.
15. **Akhmetov V.K., Shkadov V.Ya.** Atomization of a powder by a swirling flow with a recirculation zone // Fluid Dynamics. 2000. V. 35. № 6. P. 791-802.
16. **Akhmetov V.K., Akhmetova V.V.** Mathematical Modelling of Vortex Dust Separator // IOP Conf. Series: Materials Science and Engineering. 2019. 661.
17. **Akhmetov V.K., Medvedev Yu.V., Shkadov V.Ya.** Effect of the Inertia Terms in Sliding Bearing Calculation Problems // Fluid Dynamics. 2014. Vol.49. №3. P.320-329.
18. **Herrada M. A., R. Fernandez-Feria R.** On the development of three-dimensional vortex breakdown in cylindrical regions // Phys. Fluids. 2006. V. 18. 084105. 15 p.
19. **Gallaire F., Ruith M., Meiburg E., Chomaz J., Huerre P.** Spiral vortex breakdown as a global mode // J. Fluid Mech. 2006. V. 549. P. 71-80.

Vadim K. Akhmetov, Doctor of Science, Professor, Department of Computer Science and Applied Mathematics, Moscow State University of Civil Engineering, 26, Yaroslavskoe Shosse, Moscow, 129337, Russia, tel. +7(499) 183-59-94, e-mail: vadim.akhmetov@gmail.com

Ахметов Вадим Каюмович, доктор технических наук, профессор кафедры информатики и прикладной математики Национального исследовательского Московского государственного строительного университета, 129337, г. Москва, Ярославское шоссе, д. 26, тел. +7(499) 183-59-94, e-mail: vadim.akhmetov@gmail.com